Supporting Information

Temperature–induced structural transition in an organic–inorganic hybrid layered perovskite $(MA)_2PbI_{2-x}Br_x(SCN)_2$

Takuya Ohmi,[a] Tomoaki Miura,[b] Kei Shigematsu,[a,e] Alexandra A. Koegel,[c] Brian S. Newell,[d] James R. Neilson,[c] Tadaaki Ikoma,[b] Masaki Azuma,[a,e] and Takafumi Yamamoto[a]*

[a]Laboratory for Materials and Structures, Tokyo Institute of Technology, Yokohama, Kanagawa, 226–8503, Japan

[b]Graduate School of Science and Technology, Niigata University, 2–8050 Ikarashi, Nishi–ku, Niigata, 950–2181, Japan

[c]Department of Chemistry, Colorado State University, Fort Collins, Colorado 80523–1872, United States

[d]Molecular and Materials Analysis Center, Colorado State University, Fort Collins, Colorado 80523–1872, United States

[e]Kanagawa Institute of Industrial Science and Technology, 705–1 Shimoimaizumi, Ebina 243–0435, Japan

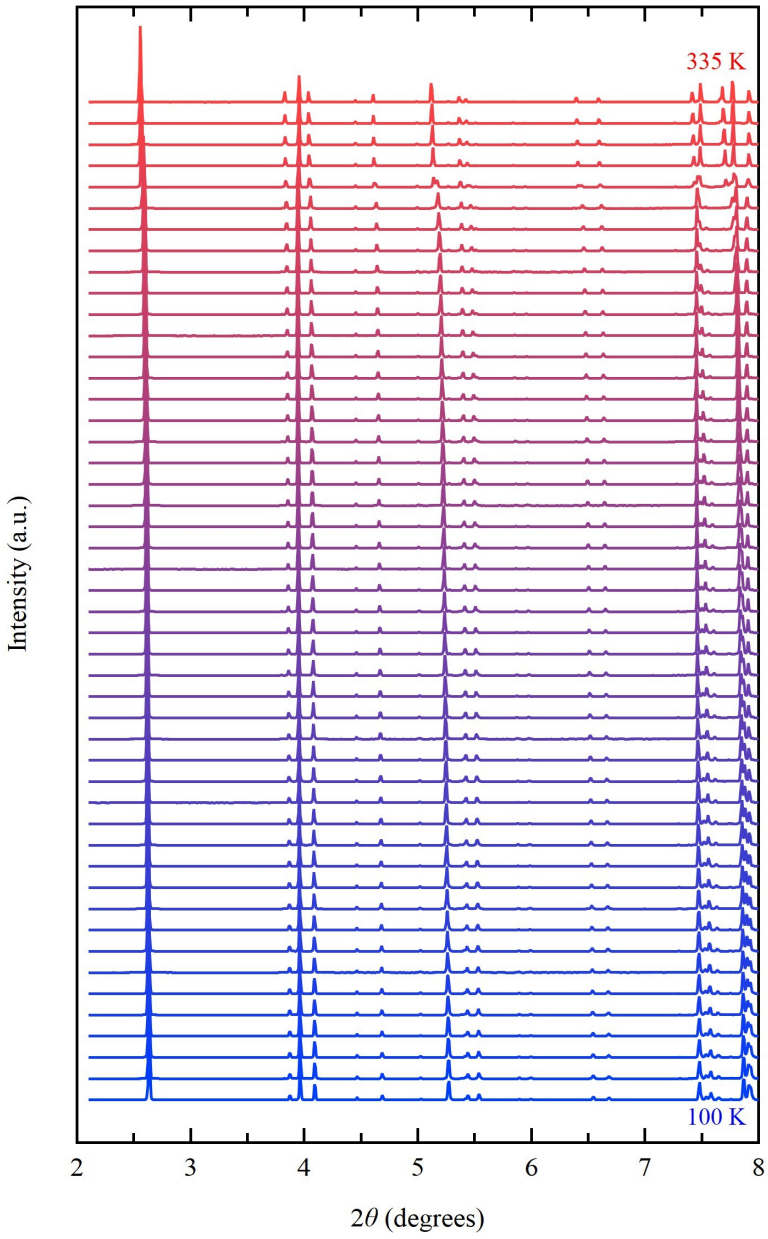

Figure S1. Temperature dependent SXRD patterns of $(MA)_2PbI_2(SCN)_2$ ($\lambda = 0.421018(1)$ Å). The patterns are showed from 100 K to 335 K at intervals of 5 K.

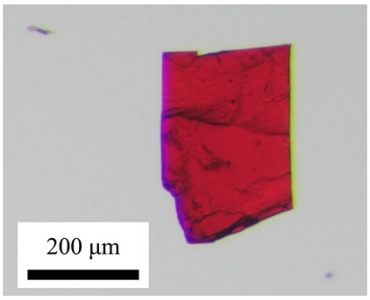

Figure S2. The photograph of $(MA)_2PbI_2(SCN)_2$ single crystal. Obtained crystal is red coloured and plate–like shaped. The surface of the crystal turns to black when the crystal is exposed to air.

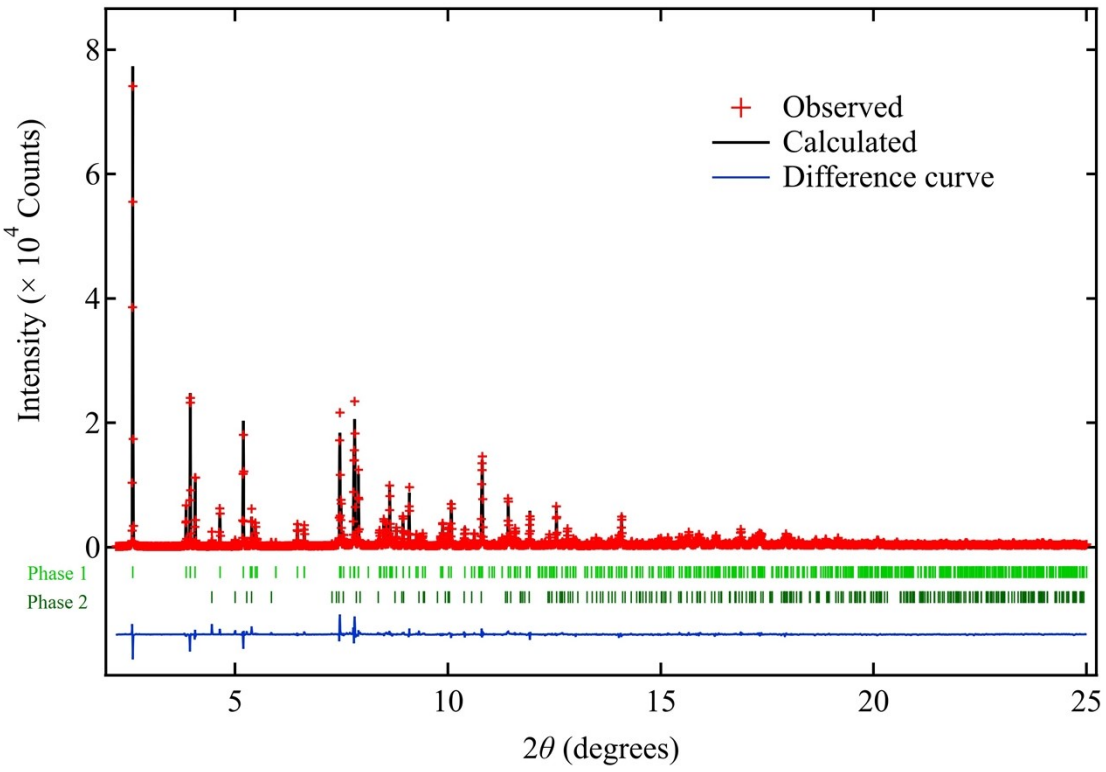

Figure S3. Representative fitting profile of Rietveld analysis of $(MA)_2PbI_2(SCN)_2$ (300 K). The refinement of the data converged with two phases, Phase 1: $(MA)_2PbI_2(SCN)_2$ and Phase 2: $Pb(SCN)_2$ (Impurity). The refined parameters are shown in Table S1.

Table S1. Crystallographic data for $(MA)_2PbI_2(SCN)_2$ obtained by synchrotron XRD data (300 K).

	atom	*g*	*x*	*y*	*z*	U_{iso} (Å^2)
Pb1	Pb	1	0.5	0.3904(3)	0.2322(4)	0.0229(5)
I1	I	1	0.5	0.8912(8)	0.2789(8)	0.044(2)
I2	I	1	0.5	0.3616(7)	-0.257(1)	0.049(1)
S1	S	1	0.339(4)	0.324(1)	0.241(4)	0.057(3)
N1	N	1	0.310538	0.561125	0.268304	0.056418
C1	C	1	0.286833	0.731423	0.296903	0.078463
N2	N	1	0.334459	0.006793	0.652103	0.070117
C2	C	1	0.356951	-0.145645	0.805004	0.077455

Space group: $Pmn2_1$; $Z = 2$; $a = 18.5927(1)$ Å, $b = 6.27010(4)$ Å, $c = 6.47344(4)$ Å. $R_p = 8.22\%$, $R_{wp} = 11.27\%$, GOF = 2.84.

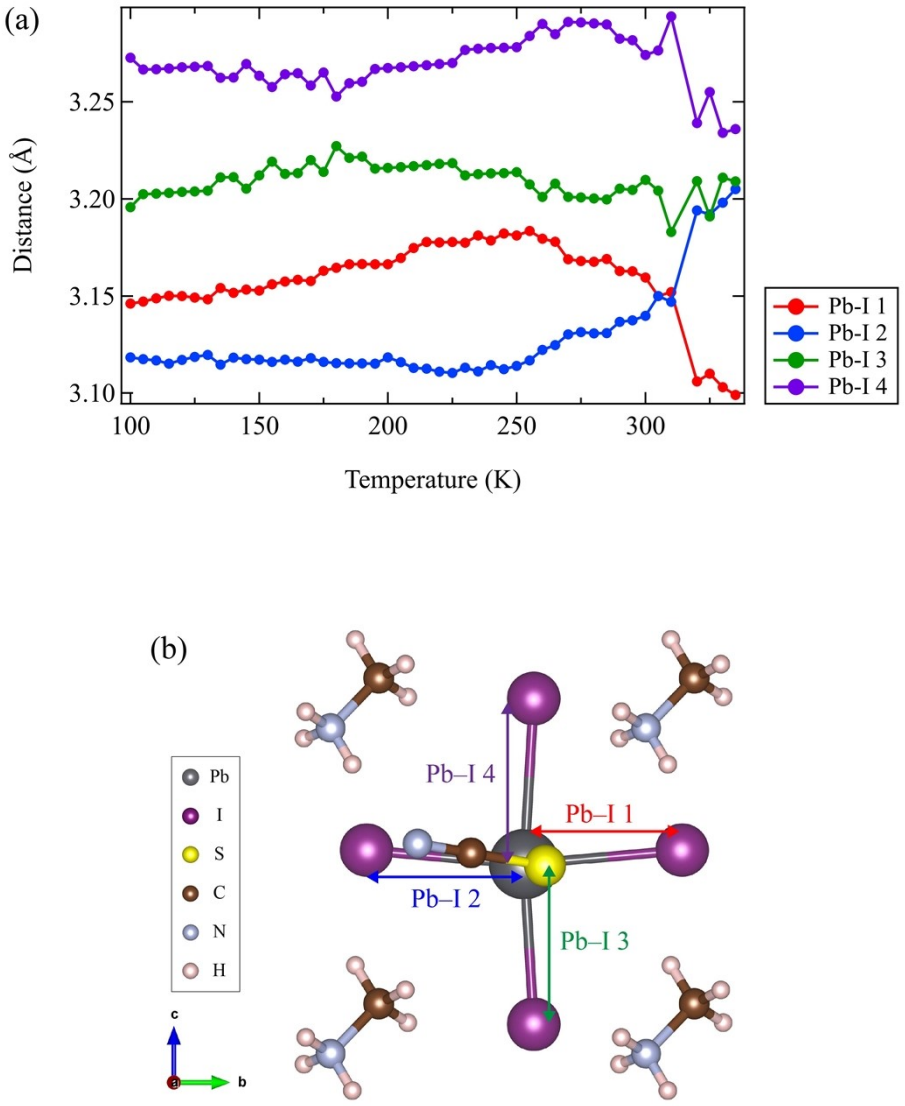

Figure S4. (a) The results of Rietveld analysis of temperature dependent SXRD data of $(MA)_2PbI_2(SCN)_2$. It reveals that atoms ate shifted at 315 K.

(b) Direction of four kinds of numbered Pb-I bonds in $(MA)_2PbI_2(SCN)_2$ lattice for reference.

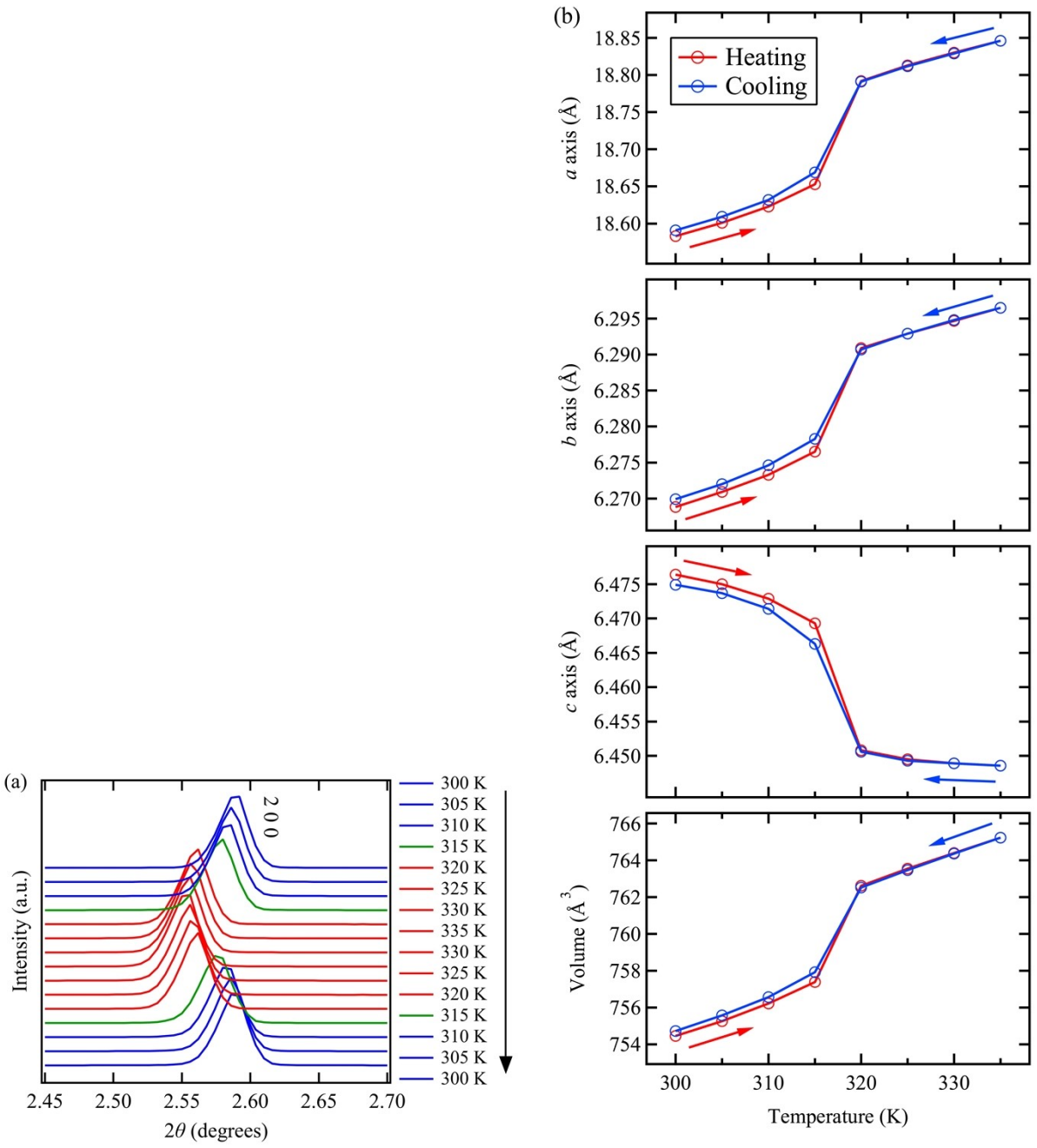

Figure S5. (a) Temperature–dependent XRD peaks from (200) plane of $(MA)_2PbI_2(SCN)_2$ during a heating and cooling cycle. The green trace at 315 K highlights the discontinuous angle shift. (b) Temperature dependence of the lattice parameters *a*, *b*, *c* and the volume of $(MA)_2PbI_2(SCN)_2$ during a heating and cooling cycle.

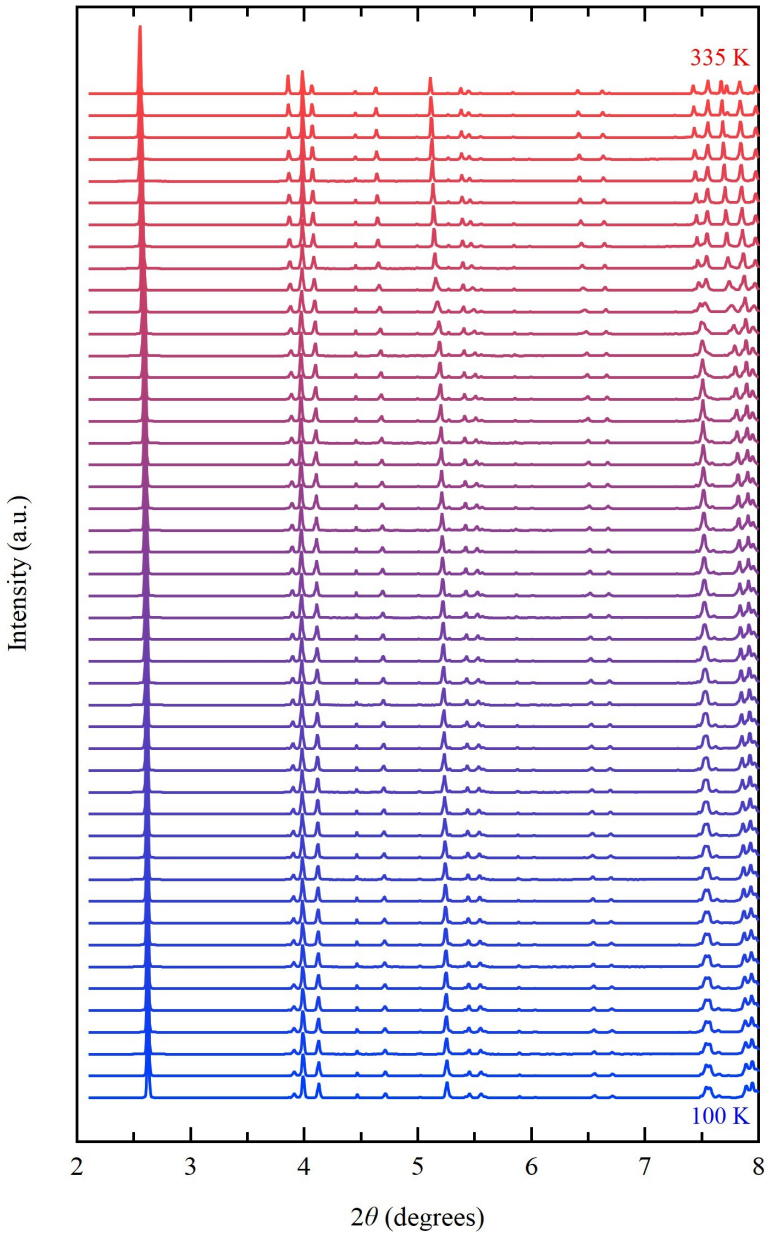

Figure S6. Temperature dependent SXRD patterns of $(MA)_2PbI_{2-x}Br_x(SCN)_2$ (x = 0.4) (λ = 0.421018(1) Å). The patterns are showed from 100 K to 335 K at intervals of 5 K.

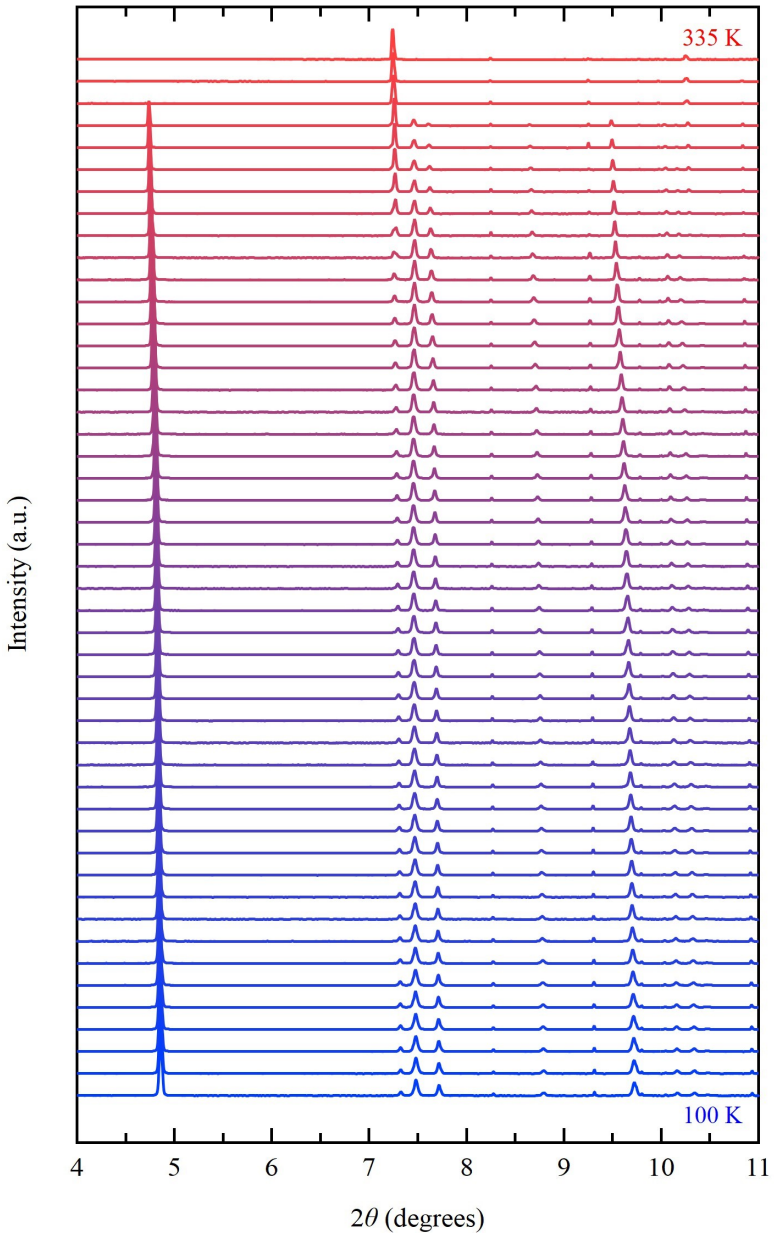

Figure S7. Temperature dependent SXRD patterns of $(MA)_2PbI_{2-x}Br_x(SCN)_2$ (x = 0.8) (λ = 0.779570(1) Å). The patterns are showed from 100 K to 335 K at intervals of 5 K.

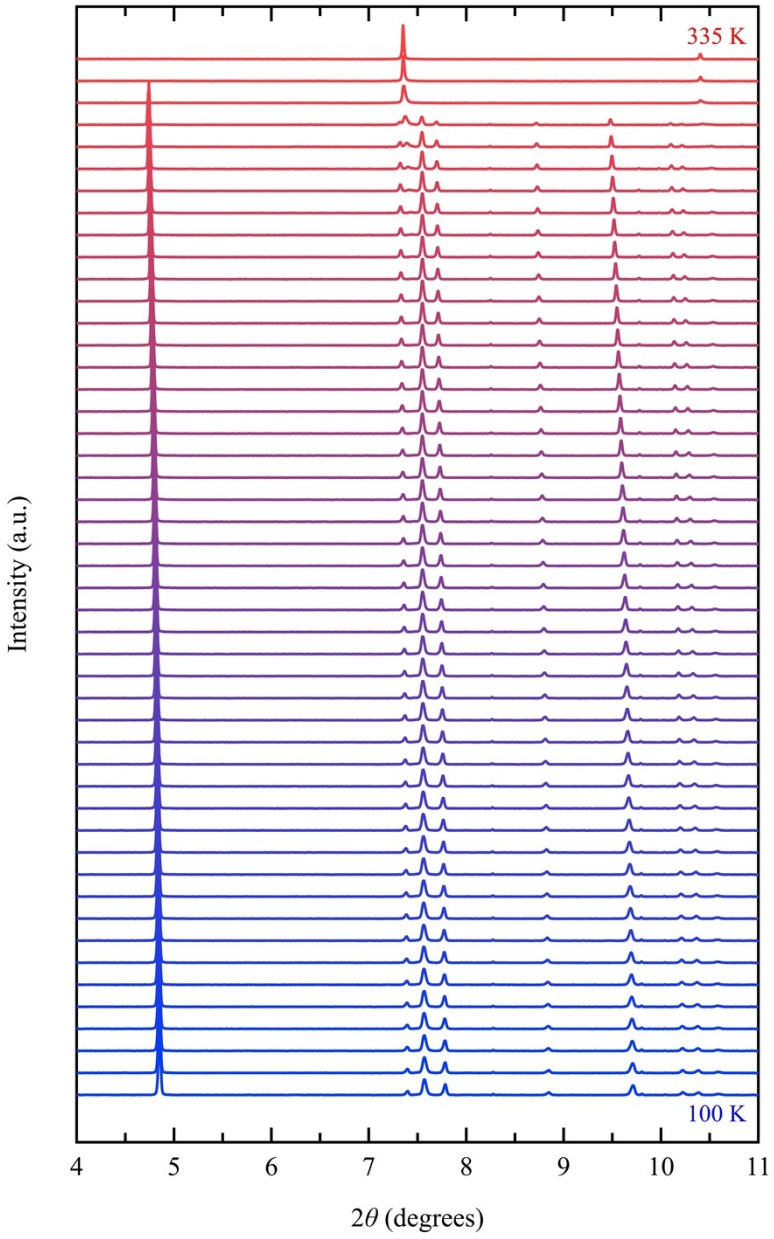

Figure S8. Temperature dependent SXRD patterns of $(MA)_2PbI_{2-x}Br_x(SCN)_2$ (x = 1.2) (λ = 0.779570(1) Å). The patterns are showed from 100 K to 335 K at intervals of 5 K.

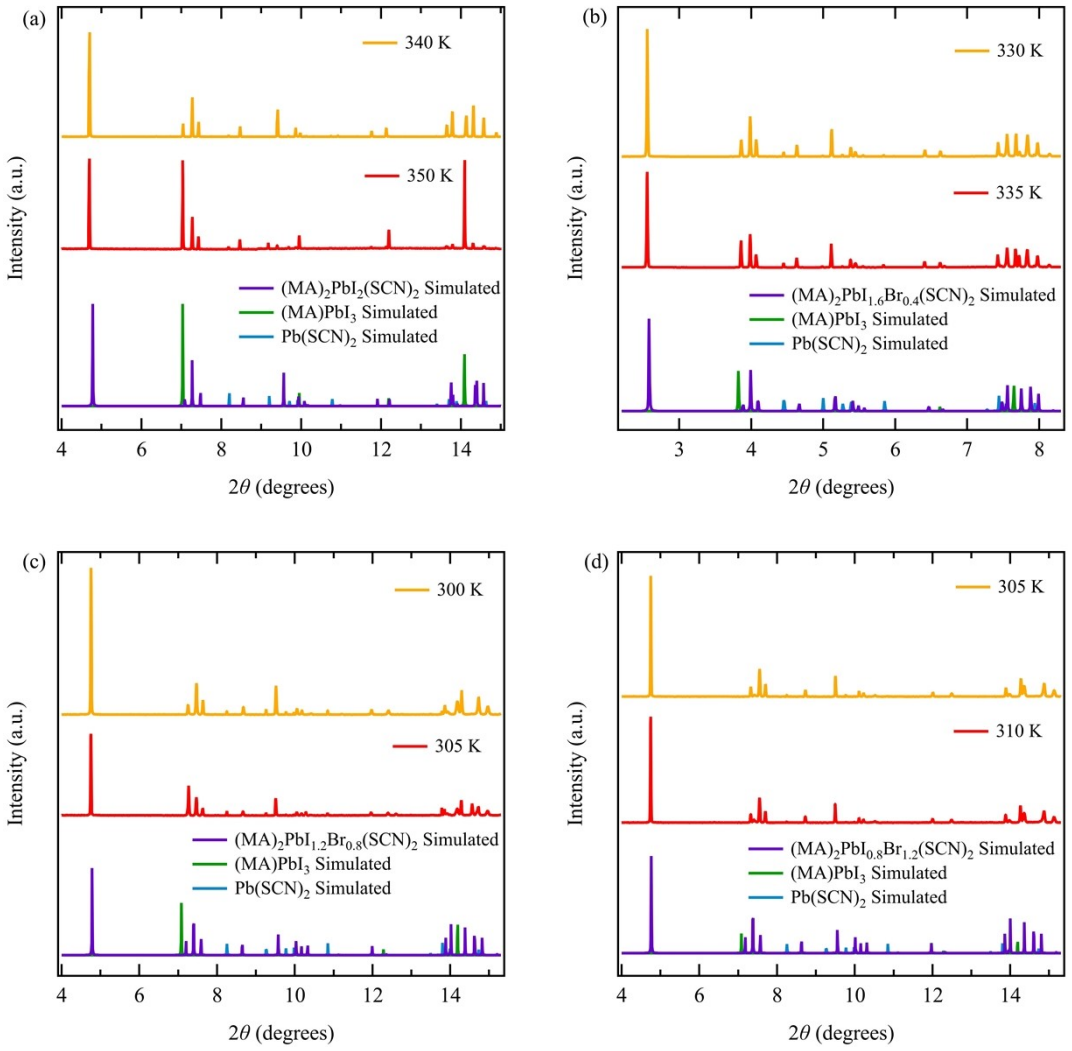

Figure S9. SXRD patterns of $(MA)_2PbI_{2-x}Br_x(SCN)_2$ around decomposition temperature. (a) x = 0 (λ = 0.774271(1) Å), (b) x = 0.4 (λ = 0.421018(1) Å), (c) x = 0.8 (λ = 0.779570(1) Å), (d) x = 1.2 (λ = 0.779570(1) Å). Decomposition temperature was determined by observation of the decrease in intensity of 200 peak with the lowest angle of $(MA)_2PbI_{2-x}Br_x(SCN)_2$. $(MA)_2PbI_{2-x}Br_x(SCN)_2$ decomposes to $MAPbI_{3-x}Br_x$ and $Pb(SCN)_2$,which agrees previous reports[1,2]. The simulated patterns of $(MA)_2PbI_{2-x}Br_x(SCN)_2$ (x = 0, 0.4) were obtained by reported single crystal X-ray structure analysis[3], and the simulated patterns of $(MA)_2PbI_{2-x}Br_x(SCN)_2$ (x = 0.8, 1.2) were calculated based on the structure of x = 0.4. The simulated patterns of $(MA)PbI_3$ (tetragonal phase;

*P*4*mm*)) and $Pb(SCN)_2$ are based on reported data.[4,5].

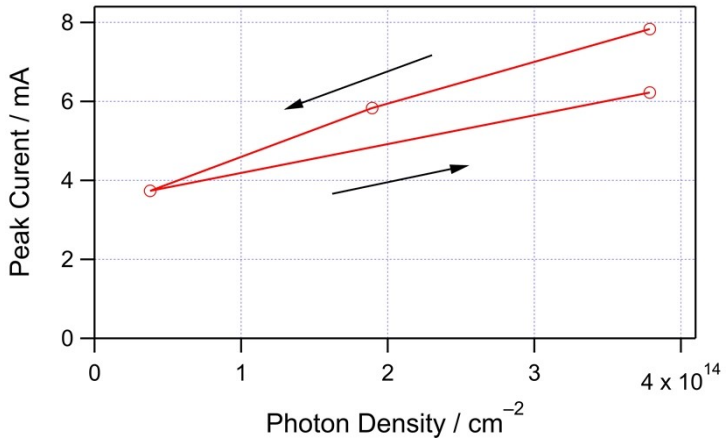

Figure S10. Dependence of initial peak photocurrent under the DC bias of 3 V on the incident photon density of the laser pulse. Black arrows indicate the measurement order. The peak current is not proportional to the photon density even allowing for the effect of degradation.

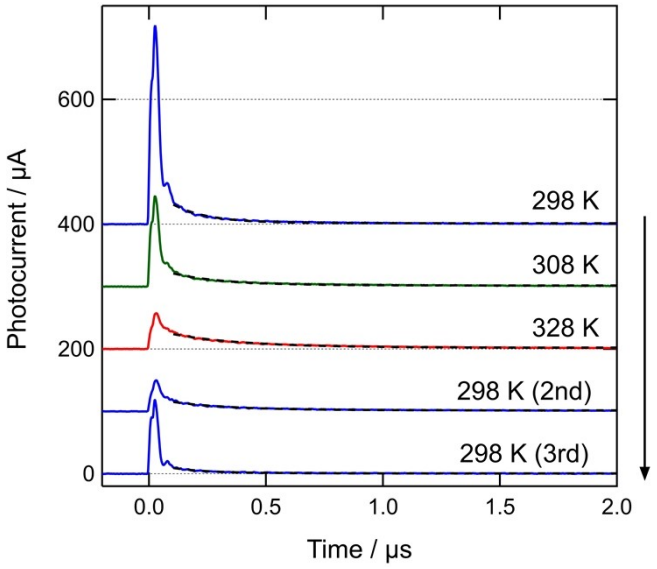

Figure S11. Temperature dependence of transient photocurrent signals. The experimental conditions other than temperature are the same with those for Figure 7 in the main text. The measurements were carried out in the order from top to bottom. The third measurement at 298 K was carried out after 1 hour of the second measurement at 298 K.

References

1 Y. Lv, D. Si, X. Song, K. Wang, S. Wang, Z. Zhao, C. Hao, L. Wei and Y. Shi, *Inorganic Chemistry*, 2018, **57**, 2045–2050.

2 D. Umeyama, Y. Lin and H. I. Karunadasa, *Chemistry of Materials*, 2016, **28**, 3241–3244.

3 T. Yamamoto, I. W. H. Oswald, C. N. Savory, T. Ohmi, A. A. Koegel, D. O. Scanlon, H. Kageyama and J. R. Neilson, *Inorganic Chemistry*, 2020, **59**, 17379–17384.

4 C. C. Stoumpos, C. D. Malliakas and M. G. Kanatzidis, *Inorganic chemistry*, 2013, **52**, 9019–38.

5 J. A. A. Mokuolu and J. C. Speakman, *Acta Crystallographica Section B Structural Crystallography and Crystal Chemistry*, 1975, **31**, 172–176.